Interaction of twisted light with many-electron atoms and ions

A. Surzhykov,[1] D. Seipt,[1] V. G. Serbo,[2,3] and S. Fritzsche[1,4]
[1]*Helmholtz-Institut Jena, D-07743 Jena, Germany*
[2]*Sobolev Institute of Mathematics, 630090 Novosibirsk, Russia*
[3]*Novosibirsk State University, 630090 Novosibirsk, Russia*
[4]*Theoretisch-Physikalisches Institut, Friedrich-Schiller-Universität Jena, D-07743 Jena, Germany*
(Received 11 November 2014; published 5 January 2015)

The excitation of many-electron atoms and ions by twisted light has been studied within the framework of the density-matrix theory and Dirac's relativistic equation. Special attention is paid to the magnetic sublevel population of excited atomic states as described by means of the alignment parameters. General expressions for the alignment of the excited states are obtained under the assumption that the photon beam, prepared as a coherent superposition of two twisted Bessel states, irradiates a macroscopic target. We demonstrate that for this case the population of excited atoms can be sensitive to both the transverse momentum and the (projection of the) total angular momentum of the incident radiation. While the expressions are general and can be employed to describe the photoexcitation of any atom, independent on its shell structure and number of electrons, we performed calculations for the $3s \rightarrow 3p$ transition in sodium. These calculations indicate that the "twistedness" of incoming radiation can lead to a measurable change in the alignment of the excited $^2P_{3/2}$ state as well as the angular distribution of the subsequent fluorescence emission.

DOI: 10.1103/PhysRevA.91.013403 PACS number(s): 32.80.−t, 31.10.+z

I. INTRODUCTION

The production and use of twisted (or vortex) light beams has been intensively discussed during the last two decades in many areas of modern physics [1–3]. In contrast to "usual" plane-wave radiation, these beams are designed to carry a *nonzero* projection of the orbital angular momentum (OAM) upon their propagation direction. The twisted photons can therefore serve as a valuable tool to better understand how the OAM influences the coupling between radiation and matter. A number of studies with vortex beams have been performed, in particular, to explore the transfer of the angular momentum to microparticles, Bose-Einstein condensates or even the bulk of semiconductors [4–6]. More recent interest, moreover, has been focused on the OAM effects in *elementary* light-matter interaction processes such as the photoionization [7,8] and scattering of twisted radiation by atoms [9,10] and free electrons [11]. In addition, a detailed theoretical analysis was carried out also for the *excitation* of atoms by vortex photon beams [12–15]. For the latter process, special emphasis was placed on the *selection rules* for the induced bound-state transitions. Both these selection rules and the sublevel population of the residual (excited) atoms were found to be strongly affected by the OAM of the incident light. It was shown, moreover, that the angular distribution and polarization of the subsequent fluorescence emission are also sensitive to the properties of the twisted radiation, thus rendering the experimental study of the OAM-induced phenomena in the atomic photoexcitation feasible.

Up to the present, however, most investigations on the excitation by vortex beams have dealt with nonrelativistic, hydrogenlike systems. Much less attention was paid to *many-electron* atoms (and ions) for which the interelectronic-interaction and relativistic effects should be taken into account. In practice, complex and especially alkali-metal atoms are the most probable candidates for future experiments on the absorption of twisted light. In order to guide these forthcoming measurements and to help to interpret their data, we present here the theoretical analysis of the photoexcitation of many-electron systems. Our study is performed within the framework of the density matrix theory, whose basic formulas are briefly reviewed in Sec. II A. In particular, we have derived the density matrix of an excited atomic state and show how it is related to the bound-bound transition amplitudes. In Sec. II B, these amplitudes are then evaluated for both incident plane-wave and twisted Bessel light. By making use of the transition amplitudes, we derive in Secs. II C and II D the *alignment* parameters which describe the magnetic sublevel population of excited atomic states. An experimental "scenario" was considered here in which the photon beam, prepared as a coherent superposition of two Bessel states with different projections of the total angular momentum (TAM), collides with a macroscopic atomic target. We show for this case that the alignment of excited atoms and the angular distribution of the subsequent fluorescent radiation are sensitive to both the TAM and (the ratio of) the transverse and longitudinal linear momenta of twisted incident beams. To illustrate the effect of "twistedness" on the photoabsorption, detailed calculations have been performed in Sec. III for the $1s^2 2s^2 2p^6 3s\ ^2S_{1/2} + \gamma \rightarrow 1s^2 2s^2 2p^6 3p\ ^2P_{3/2}$ transition in sodium atom. Finally, a summary of our results and a short outlook are given in Sec. IV.

Hartree atomic units ($\hbar = e = m_e = 1, c = 1/\alpha$) are used throughout the paper unless stated otherwise.

II. THEORY

A. Density-matrix formalism

The formation of excited atomic states in collisions with ions, electrons, or photons is described most conveniently within the framework of the density-matrix theory [16,17]. In this approach, the overall system "target atom + projectile" before and after the collision process is described by an initial

$\hat{\rho}_i$ and final $\hat{\rho}_f$ statistical (or density) operators, respectively. These operators are connected by the transition operator $\hat{\mathcal{T}}$ which describes the interaction.

If a photon is absorbed by an atom, an initial state of the overall system comprises (i) the incoming photon beam and (ii) an atom in the state $|\alpha_i J_i\rangle$ with well-defined total angular momentum J_i, and where α_i is used to denote all additional quantum numbers. Therefore, the (initial-state) statistical operator $\hat{\rho}_i$ can be written as a direct product of the atomic, $\hat{\rho}_i^{\rm A}$, and photonic, $\hat{\rho}^{\rm ph}$, operators:

$$\hat{\rho}_i = \hat{\rho}_i^{\rm A} \otimes \hat{\rho}^{\rm ph}. \tag{1}$$

For initially unpolarized target atoms, moreover, the (atomic) statistical operator $\hat{\rho}_i^{\rm A}$ reads

$$\hat{\rho}_i^{\rm A} = \frac{1}{2J_i+1} \sum_{M_i} |\alpha_i J_i M_i\rangle\langle \alpha_i J_i M_i|, \tag{2}$$

where the summation runs over the magnetic quantum number, $-J_i \leqslant M_i \leqslant J_i$.

By using the initial-state statistical operator (1), we can find the final operator:

$$\hat{\rho}_f = \hat{\mathcal{T}}\, \hat{\rho}_i\, \hat{\mathcal{T}}^\dagger, \tag{3}$$

that describes the atom in the excited state $|\alpha_f J_f\rangle$, and where $\hat{\mathcal{T}}$ characterizes the interaction of the electrons with the radiation field. The detailed representation of the *transition* operator $\hat{\mathcal{T}}$ depends on the state in which the incident light is prepared. In the next section we shall consider, for example, the interaction of atoms with the plane-wave and twisted light.

For a further analysis of the absorption process, it is convenient to rewrite Eq. (3) in *matrix* form:

$$\begin{aligned}
&\langle \alpha_f J_f M_f|\hat{\rho}_f|\alpha_f J_f M_f'\rangle \\
&\quad = \frac{1}{2J_i+1} \sum_{M_i} \langle \gamma_i|\hat{\rho}^{\rm ph}|\gamma_i\rangle \langle \alpha_f J_f M_f|\hat{\mathcal{T}}|\alpha_i J_i M_i, 1_{\gamma_i}\rangle \\
&\qquad \times \langle \alpha_i J_i M_i, 1_{\gamma_i}|\hat{\mathcal{T}}^\dagger|\alpha_f J_f M_f'\rangle,
\end{aligned} \tag{4}$$

where we have used Eqs. (1) and (2) and where γ_i denotes the set of quantum numbers to specify the state of the photon. As seen from this expression, the final-state density matrix depends on the polarization (spin) state of the incoming photons as well as on the amplitude $\langle \alpha_f J_f M_f|\hat{\mathcal{T}}|\alpha_i J_i M_i, 1_{\gamma_i}\rangle$ as associated with the atomic absorption process, $|\alpha_i J_i M_i\rangle + \gamma_i \to |\alpha_f J_f M_f\rangle$. The evaluation of this transition matrix element will be discussed in the next sections.

B. Evaluation of the transition amplitude

As shown above, the calculation of the final-state density matrix (4) can be traced back to the matrix element of the transition operator $\hat{\mathcal{T}}$. Within the relativistic framework and for *many-electron* atom or ion, this matrix element can be written as [18,19]

$$\begin{aligned}
&\langle \alpha_f J_f M_f|\hat{\mathcal{T}}|\alpha_i J_i M_i, 1_{\gamma_i}\rangle \\
&\quad = C\, \langle \alpha_f J_f M_f| \sum_q \boldsymbol{\alpha}_q \boldsymbol{A}_{\gamma_i}(\boldsymbol{r}_q)|\alpha_i J_i M_i\rangle.
\end{aligned} \tag{5}$$

Here, the q runs over all electrons in a target atom, $\boldsymbol{\alpha}_q$ denotes the vector of Dirac matrices for the qth particle, and the proportionality coefficient C can be determined from the standard normalization condition $\mathrm{Tr}(\hat{\rho}_f) = 1$ of the density matrix. In Eq. (5), moreover, the $\boldsymbol{A}_{\gamma_i}(\boldsymbol{r})$ is the vector potential of the electromagnetic field. In order to further simplify the transition amplitude we need to agree first about explicit form of the $\boldsymbol{A}_{\gamma_i}(\boldsymbol{r})$.

1. Photon vector potential

In atomic physics, one usually assumes that an atom interacts with a *plane-wave* radiation with a wave vector $\boldsymbol{k}$, energy $\omega = k/\alpha$, and helicity $\lambda = \pm 1$. For this—standard—case, the vector potential $\boldsymbol{A}_{\gamma_i}(\boldsymbol{r}) = \boldsymbol{A}^{\rm (pl)}_{\boldsymbol{k}\lambda}(\boldsymbol{r})$ is given by

$$\boldsymbol{A}^{\rm (pl)}_{\boldsymbol{k}\lambda}(\boldsymbol{r}) = \boldsymbol{e}_{\boldsymbol{k}\lambda}\, e^{i\boldsymbol{k}\boldsymbol{r}}, \tag{6}$$

where $\boldsymbol{e}_{\boldsymbol{k}\lambda}$ is the polarization vector (as defined, e.g., in Ref. [8]). For the further analysis of the transition amplitude (5) it is practical to decompose the vector potential $\boldsymbol{A}^{\rm (pl)}_{\boldsymbol{k}\lambda}(\boldsymbol{r})$ in terms of its electric and magnetic multipole fields. If the propagation direction of the light $\hat{\boldsymbol{k}} = \boldsymbol{k}/k = (\theta_k, \varphi_k, 0)$ does not coincide with the quantization (z) axis, this decomposition reads as [20]

$$\begin{aligned}
\boldsymbol{e}_{\boldsymbol{k}\lambda}\, \mathrm{e}^{i\boldsymbol{k}\boldsymbol{r}} &= \sqrt{2\pi} \sum_{LM} \sum_{p=0,1} i^L\, [L]^{1/2}\, (i\lambda)^p \\
&\quad \times D^L_{M\lambda}(\varphi_k, \theta_k, 0)\, \boldsymbol{a}^p_{LM}(\boldsymbol{r}),
\end{aligned} \tag{7}$$

where $[L] = 2L+1$, $D^L_{M\lambda}$ is the Wigner rotation matrix, and $\boldsymbol{a}^p_{LM}(\boldsymbol{r})$ refers to magnetic ($p = 0$) and electric ($p = 1$) multipole components, respectively. For the sake of brevity, we will not present here the explicit form of these components and refer the reader instead to Refs. [19–21].

If, instead of plane waves (6), we shall study the interaction of atomic target with *twisted* light; we have to use the vector potential $\boldsymbol{A}_{\gamma_i}(\boldsymbol{r}) = \mathbf{A}^{(1,\mathrm{tw})}_{\varkappa m k_z \lambda}(\boldsymbol{r})$ in Eq. (5). This potential describes light with a well-defined helicity λ, longitudinal component k_z of the linear momentum, and the projection m of the total angular momentum (TAM) upon the quantization (z) axis. We will assume, moreover, that the (absolute value of) transverse momentum $|\boldsymbol{k}_\perp| = \varkappa$ and, hence, the photon energy $\omega = k/\alpha = \sqrt{k_z^2 + \varkappa^2}/\alpha$ are fixed. Light in such a quantum state is usually referred to as a *Bessel* beam, and is characterized by the vector potential [8,11,15]

$$\mathbf{A}^{(1,\mathrm{tw})}_{\varkappa m k_z \lambda}(\boldsymbol{r}) = \int \boldsymbol{e}_{\boldsymbol{k}\lambda}\, \mathrm{e}^{i\boldsymbol{k}\boldsymbol{r}} a_{\varkappa m}(\boldsymbol{k}_\perp)\, \frac{d^2 k_\perp}{(2\pi)^2}, \tag{8}$$

where the amplitude $a_{\varkappa m}(\boldsymbol{k}_\perp)$ is given by

$$a_{\varkappa m}(\boldsymbol{k}_\perp) = (-i)^m\, e^{im\phi_k} \sqrt{\frac{2\pi}{k_\perp}}\, \delta(k_\perp - \varkappa). \tag{9}$$

As follows from this expression, the twisted (Bessel) beam can be *seen* in momentum space as a coherent superposition of plane waves whose wave vectors $\boldsymbol{k}$ are uniformly distributed upon the surface of a cone with a polar opening angle $\theta_k = \arctan(\varkappa/k_z)$ and the (cone) axis in the z direction. Such Bessel photons can be easily generated experimentally. Owing to recent developments in the manipulation of optical beams,

in addition, different Bessel beams with the same kinematic parameters $(\varkappa, k_z)$ but different projections of the total angular momentum can be superimposed and used in experiments. In order to describe the interaction of such a "tailored" radiation with an atom, we therefore construct the vector potential

$$\mathbf{A}^{(2,\mathrm{tw})}(\boldsymbol{r}) = c_1\, \mathbf{A}^{(1,\mathrm{tw})}_{\varkappa m_1 k_z \lambda}(\boldsymbol{r}) + c_2\, \mathbf{A}^{(1,\mathrm{tw})}_{\varkappa m_2 k_z \lambda}(\boldsymbol{r}), \tag{10}$$

where

$$c_n = |c_n| e^{i\alpha_n}, \quad |c_1|^2 + |c_2|^2 = 1. \tag{11}$$

To be more specific, we consider here a coherent superposition of two Bessel beams with different projections $m_{1,2}$ of the total angular momentum but with the same helicity λ and the same beam axis.

2. Radiative matrix element

Having briefly discussed the properties of the vector potential for the plane-wave and twisted radiation, we are ready now to further evaluate the many-particle transition amplitude (5). If we assume that the incident light is prepared in the *pure* quantum-mechanical state $|\gamma_i\rangle$, described by Eq. (10), we obtain

$$\begin{aligned}
&\langle \alpha_f J_f M_f | \hat{\mathcal{T}} | \alpha_i J_i M_i, 1_{\gamma_i} \rangle \\
&\quad = C \langle \alpha_f J_f M_f | \sum_q \boldsymbol{\alpha}_q\, \mathbf{A}^{(2,\mathrm{tw})}(\boldsymbol{r}_q) | \alpha_i J_i M_i \rangle \\
&\quad = C \sum_{n=1,2} c_n \langle \alpha_f J_f M_f | \sum_q \boldsymbol{\alpha}_q \mathbf{A}^{(1,\mathrm{tw})}_{\varkappa m_n k_z \lambda}(\boldsymbol{r}_q) | \alpha_i J_i M_i \rangle .
\end{aligned} \tag{12}$$

By inserting the decomposition (8) of the twisted vector potential $\mathbf{A}^{(1,\mathrm{tw})}_{\varkappa m_n k_z \lambda}(\boldsymbol{r})$ into this expression one finds

$$\begin{aligned}
&\langle \alpha_f J_f M_f, 0 | \hat{\mathcal{T}} | \alpha_i J_i M_i, 1_{\gamma_i} \rangle = C \sum_{n=1,2} c_n \\
&\times \int a_{\varkappa m_n}(\boldsymbol{k}_\perp)\, e^{-i \boldsymbol{k}_\perp \boldsymbol{b}}\, \langle \alpha_f J_f M_f | \hat{\mathcal{R}}_\lambda(\boldsymbol{k}) | \alpha_i J_i M_i \rangle \frac{d^2 k_\perp}{(2\pi)^2},
\end{aligned} \tag{13}$$

where the many-particle operator

$$\hat{\mathcal{R}}_\lambda(\boldsymbol{k}) = \sum_q \boldsymbol{\alpha}_q\, \boldsymbol{e}_{\boldsymbol{k}\lambda}\, e^{i \boldsymbol{k} \boldsymbol{r}_q} \tag{14}$$

describes the interaction of electrons with the plane-wave radiation field. In Eq. (13), moreover, an additional exponential factor $\exp(-i \boldsymbol{k}_\perp \boldsymbol{b})$ is introduced to specify the lateral position of a target atom with regard to the beam axis of the incident light, and where the impact parameter $\boldsymbol{b} = (b_x, b_y, 0)$.

Equation (13) shows how the computation of the $\mathcal{T}$ amplitude for the incident twisted light can be made by using the well-known matrix elements $\langle \alpha_f J_f M_f | \hat{\mathcal{R}}_\lambda(\boldsymbol{k}) | \alpha_i J_i M_i \rangle$ for the absorption of *plane-wave* photons that propagate along the direction $\hat{\boldsymbol{k}} = (\theta_k, \varphi_k)$ with respect to the quantization axis. By employing the multipole expansion (7) of the photon vector potential, we find

$$\begin{aligned}
&\langle \alpha_f J_f M_f | \hat{\mathcal{R}}_\lambda(\boldsymbol{k}) | \alpha_i J_i M_i \rangle \\
&\quad \equiv \langle \alpha_f J_f M_f | \sum_q \boldsymbol{\alpha}_q\, \boldsymbol{e}_{\boldsymbol{k}\lambda}\, e^{i \boldsymbol{k} \boldsymbol{r}_q} | \alpha_i J_i M_i \rangle \\
&\quad = \sqrt{2\pi} \sum_{LM} \sum_{p=0,1} i^L \frac{[L]^{1/2}}{[J_f]^{1/2}} (i\lambda)^p\, D^L_{M\lambda}(\theta_k, \varphi_k, 0) \\
&\qquad \times \langle J_i M_i\, LM | J_f M_f \rangle\, \langle \alpha_f J_f || H_\gamma(pL) || \alpha_i J_i \rangle,
\end{aligned} \tag{15}$$

where, in the last line, we made use of the Wigner-Eckart theorem and introduced the notation

$$\langle \alpha_f J_f || H_\gamma(pL) || \alpha_i J_i \rangle = \left\langle \alpha_f J_f \left\| \sum_q \boldsymbol{\alpha}_q\, \boldsymbol{a}^p_{L,q} \right\| \alpha_i J_i \right\rangle \tag{16}$$

for the many-electron *reduced* matrix element. This (reduced) matrix element forms the "building block" to describe all the properties of the photoabsorption process. An efficient evaluation of the $\langle \alpha_f J_f || H_\gamma(pL) || \alpha_i J_i \rangle$ within the framework of the multiconfiguration Dirac-Fock theory has been discussed previously [22].

C. Statistical tensors of excited atomic states

Having derived the transition amplitude (13)–(15), we can further evaluate the final-state density matrix (4). Instead of this matrix, however, it is often more convenient to describe the population of photoexcited atomic states in terms of the so-called statistical tensors:

$$\begin{aligned}
\rho_{k_f q_f}(\alpha_f J_f) = \sum_{M_f M'_f} (-1)^{J_f - M'_f}\, &\langle J_f M_f\, J_f - M'_f | k_f q_f \rangle \\
&\times \langle \alpha_f J_f M_f | \hat{\rho}_f | \alpha_f J_f M'_f \rangle,
\end{aligned} \tag{17}$$

which transform like the spherical harmonics of rank k_f under a rotation of the coordinates. Owing to the properties of the Clebsch-Gordan coefficients $\langle \ldots | \ldots \rangle$, nonzero tensor components arise only for integer values of the *rank* $0 \leqslant k_f \leqslant 2J_i$ and the *projection* $-k_f \leqslant q_f \leqslant k_f$. Moreover, if the density matrix is diagonal in the $|\alpha_f J_f M_f\rangle$ basis, the relation $\rho_{k_f q_f}(\alpha_f J_f) = \delta_{q_f 0}\, \rho_{k_f 0}(\alpha_f J_f)$ holds.

The final-state density matrix $\hat{\rho}_f$ and, hence, the statistical tensors (17) depend on the impact parameter $\boldsymbol{b}$ which describes the position of a target atom in the twisted wavefront. If a Bessel beam with radius R collides with a *macroscopic* target of randomly distributed atoms, we have to average over the $\boldsymbol{b}$:

$$\begin{aligned}
\rho^{(\mathrm{tw})}_{k_f q_f}(\alpha_f J_f) = C \sum_{M_i} \sum_{M_f M'_f} (-1)^{J_f - M'_f}\, &\langle J_f M_f\, J_f - M'_f | k_f q_f \rangle \sum_{n,n'=1,2} |c_n|\, |c'_n|\, e^{i(\alpha_n - \alpha'_n)} \\
&\times \int a_{\varkappa m_n}(\boldsymbol{k}_\perp)\, a^*_{\varkappa m_{n'}}(\boldsymbol{k}'_\perp)\, e^{i(\boldsymbol{k}'_\perp - \boldsymbol{k}_\perp)\boldsymbol{b}} \langle \alpha_f J_f M_f | \hat{\mathcal{R}}_\lambda(\boldsymbol{k}) | \alpha_i J_i M_i \rangle \langle \alpha_f J_f M'_f | \hat{\mathcal{R}}_\lambda(\boldsymbol{k}') | \alpha_i J_i M_i \rangle^* \frac{d^2 k_\perp}{(2\pi)^2} \frac{d^2 k'_\perp}{(2\pi)^2} \frac{d^2 \boldsymbol{b}}{\pi R^2}.
\end{aligned} \tag{18}$$

In this expression, moreover, we used Eqs. (4) and (13). In order to further evaluate the statistical tensors (18) one needs to apply the expression (9) for the amplitudes $a_{\varkappa m_n}(\boldsymbol{k}_\perp)$ and to perform the integration over the $\boldsymbol{b}$ as well as the transverse momenta $\boldsymbol{k}_\perp$ and $\boldsymbol{k}'_\perp$:

$$\rho^{(\mathrm{tw})}_{k_f q_f}(\alpha_f J_f) = C \sum_{M_i} \sum_{M_f M'_f} (-1)^{J_f - M'_f} \langle J_f M_f \, J_f - M'_f | k_f q_f \rangle \sum_{n,n'=1,2} |c_n| \, |c'_n| \, e^{i(\alpha_n - \alpha'_n)} \, i^{m_n - m'_n}$$
$$\times \int e^{i(m_n - m'_n)\varphi_k} \langle \alpha_f J_f M_f | \hat{\mathcal{R}}_\lambda(\boldsymbol{k}) | \alpha_i J_i M_i \rangle \langle \alpha_f J_f M'_f | \hat{\mathcal{R}}_\lambda(\boldsymbol{k}) | \alpha_i J_i M_i \rangle^* \frac{d\varphi_k}{2\pi}. \tag{19}$$

The remaining φ_k integration can be readily carried out by using the multipole expansion of the plane-wave matrix elements (15) and by making some simple angular momentum algebra:

$$\rho^{(\mathrm{tw})}_{k_f q_f}(\alpha_f J_f) = \rho^{(\mathrm{pl})}_{k_f 0}(\alpha_f J_f) \left(\delta_{q_f,0} \, P_{k_f}(\cos\theta_k) + \sum_{n \neq n'} |c_n| |c'_n| \, e^{i \, \Delta_{nn'}} \, \delta_{q_f, \, m_n - m_{n'}} \, d^{k_f}_{q_f 0}(\theta_k) \right), \tag{20}$$

where $\Delta_{nn'} = \alpha_n - \alpha_{n'} + \frac{\pi}{2}(m_{n'} - m_n)$, $P_{k_f}(\cos\theta_k)$ is the Legendre polynomial, and where the tensor $\rho^{(\mathrm{pl})}_{k_f 0}(\alpha_f J_f)$ describes the sublevel population following the absorption of a *plane-wave* photon with helicity λ:

$$\rho^{(\mathrm{pl})}_{k_f 0}(\alpha_f J_f) = C \sum_{LL' pp'} i^{L+L'} \, [L, L']^{1/2} \, (i\lambda)^p \, (-i\lambda)^{p'} (-1)^{L' + J_f + J_i + k_f} \, \langle L \lambda L' - \lambda | k_f 0 \rangle$$
$$\times \begin{Bmatrix} L & L' & k_f \\ J_f & J_f & J_i \end{Bmatrix} \langle \alpha_f J_f || H_\gamma(pL) || \alpha_i J_i \rangle \, \langle \alpha_f J_f || H_\gamma(p' L') || \alpha_i J_i \rangle^*. \tag{21}$$

Indeed, expression (20) represents the general form of the statistical tensors of an excited atomic state following the photoabsorption from a coherent superposition of two Bessel beams (10). Below we will discuss in detail the dependence of these tensors on the "twistedness" of incident light. First, however, let us consider how $\rho_{k_f q_f}$ can be used in order to calculate the angular distribution of the subsequent radiative decay $|\alpha_f J_f\rangle \to |\alpha_0 J_0\rangle + \gamma$ to one of the lower-lying levels.

D. Angular properties of the fluorescent radiation

Since the angular distribution of the characteristic radiation has been discussed very frequently in the past, we may restrict ourselves to a rather short account of basic formulas and refer for all further details to Refs. [17,23]. In the density-matrix approach, the emission pattern of the decay photons is closely related to *reduced* statistical tensors of an excited state:

$$\mathcal{A}_{k_f q_f}(\alpha_f J_f) = \frac{\rho_{k_f q_f}(\alpha_f J_f)}{\rho_{00}(\alpha_f J_f)}, \tag{22}$$

and which are often referred to as alignment or orientation parameters. These parameters are independent of the particular normalization of the density matrix and describe the relative population of atomic sublevels $|\alpha_f J_f M_f\rangle$. The alignment parameters (22) with zero projection $q_f = 0$ are directly expressed in terms of the partial cross sections $\sigma_{\alpha_F J_f M_f} \equiv \sigma_{M_f}$ for the excitation to a particular magnetic state. For example, the parameter

$$\mathcal{A}_{20}(J_f = 3/2) = \frac{\sigma_{3/2} + \sigma_{-3/2} - \sigma_{1/2} - \sigma_{-1/2}}{\sigma_{3/2} + \sigma_{-3/2} + \sigma_{1/2} + \sigma_{-1/2}} \tag{23}$$

simply describes the population of a level with $J_f = 3/2$. Unfortunately, no simple expressions can be written for the reduced statistical tensors $\mathcal{A}_{k_f q_f}(\alpha_f J_f)$ with $q_f \neq 0$; these tensors are generally complex and characterize the coherence between sublevels with different M_f.

Using the reduced statistical tensors, the angular distributions of the $|\alpha_f J_f\rangle \to |\alpha_0 J_0\rangle + \gamma$ fluorescence light can be written as

$$W_{\mathrm{dec}}(\theta) = \frac{1}{4\pi} \left(1 + \sum_{k_f = 2,4,\ldots} \sum_{q_f = -k_f}^{k_f} \sqrt{\frac{4\pi}{2k_f + 1}} \, Y_{k_f q_f}(\theta, 0) \right.$$
$$\left. \times \, \mathcal{A}_{k_f q_f}(\alpha_f J_f) \, f_{k_f}(\alpha_f J_f, \alpha_0 J_0) \right), \tag{24}$$

where the angle θ is defined with respect to the propagation direction of the incident twisted beam; cf. Fig. 1. We see from this expression that, apart from the alignment of the excited state, the $W_{\mathrm{dec}}(\theta)$ depends also on the so-called *structure functions* $f_{k_f}(\alpha_f J_f, \alpha_0 J_0)$. These functions are independent of the formation of the excited state $|\alpha_f J_f\rangle$ and merely reflect the electronic structure of an atom. The general expression for the $f_{k_f}(\alpha_f J_f, \alpha_0 J_0)$ is rather complicated and contains the

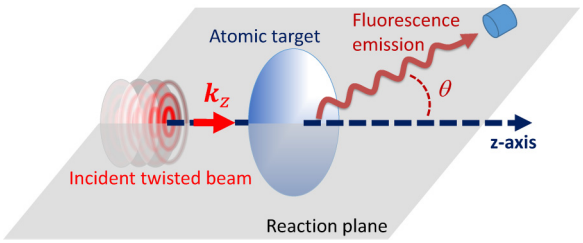

FIG. 1. (Color online) Geometry for the excitation of atoms by twisted light and for the subsequent fluorescence emission. The quantization (z) axis is chosen along the propagation direction of the incoming Bessel photons. This axis also defines, together with the direction of the fluorescence emission, the reaction (xz) plane.

summation over different multipole channels that are allowed for a particular radiative transition (see, e.g., Refs. [21,23,24]). Within the leading electric dipole ($E1$) approximation, however, the structure function can be simplified to

$$f_{k_f}(\alpha_f J_f, \alpha_0 J_0) = \delta_{k_f,2}\,(-1)^{1+J_f+J_0}\sqrt{\frac{3(2J_f+1)}{2}} \times \begin{Bmatrix} 1 & 1 & 2 \\ J_f & J_f & J_0 \end{Bmatrix}, \tag{25}$$

and, thus, restricts the summation in Eq. (24) to the terms with $k_f = 2$. In the $E1$ approximation, therefore, only the second-rank alignment parameters $\mathcal{A}_{2q_f}$ with $-2 \leqslant q_f \leqslant +2$ can affect the angular distribution of the fluorescent photons.

III. RESULTS AND DISCUSSION

In the previous section we have derived the general expressions (20)–(22) for the reduced statistical tensors of the excited atomic state $|\alpha_f J_f\rangle$ following the absorption of twisted light. In particular, this light was "constructed" as a coherent superposition of two Bessel beams with opening angle θ_k and the TAM projections m_1 and m_2. Below we will investigate how these particular properties of the incident (twisted) light affect the alignment of excited atoms *and* the angular distribution of the subsequent characteristic fluorescence. In order to perform such an analysis we have to agree first about the geometry under which the photoabsorption and fluorescence emission is observed. As seen from Fig. 1, we choose the quantization axis of the overall system along the direction of propagation of the Bessel beam. The xz- (reaction) plane is spanned then by the k_z and the wave vector $\boldsymbol{k}_{\rm dec}$ of the decay photons.

A. Absorbing photons from a single Bessel beam

We start our discussion about the population of photoexcited atomic states from the simplest scenario in which a *single* Bessel beam interacts with an initially unpolarized target. By implying $c_1 = 1$ and $c_2 = 0$ in Eqs. (20) and (22) we immediately obtain for the reduced statistical tensors

$$\mathcal{A}^{(1,\rm tw)}_{k_f q_f}(\alpha_f J_f) = \delta_{q_f,0}\, P_{k_f}(\cos\theta_k)\, \mathcal{A}^{(\rm pl)}_{k_f 0}(\alpha_f J_f), \tag{26}$$

and where $\mathcal{A}^{(\rm pl)}_{k_f 0}$ describes the alignment of the atom following the absorption of circularly polarized, plane-wave radiation. As seen from this formula, the parameters $\mathcal{A}^{(1,\rm tw)}_{k_f q_f}(\alpha_f J_f)$ are independent on the projection of the TAM of light and are sensitive only to the opening angle θ_k. Moreover, the reduced statistical tensors with nonzero projections $q_f \neq 0$ vanish identically, thus, indicating that the excited atomic states possess axial symmetry with respect to the propagation direction of the beam, i.e., the quantization (z) axis. This symmetry behavior can be well understood if we note that the overall system in the initial state consists of an unpolarized atom and an incident Bessel beam with an axially symmetric transverse energy density profile $\rho(x,y)$ [see Fig. 3(a)].

In order to illustrate the θ_k behavior of the alignment of excited atomic states we consider the $3s$-$3p$ excitation of atomic sodium. This "yellow" $3s\,^2S_{1/2}\,(J_i = 1/2) \rightarrow\ 3p\,^2P_{3/2}\,(J_f = 3/2)$ transition can be induced by twisted photons with energy $\hbar\omega = 2.104$ eV and helicity $\lambda = +1$. For this transition,

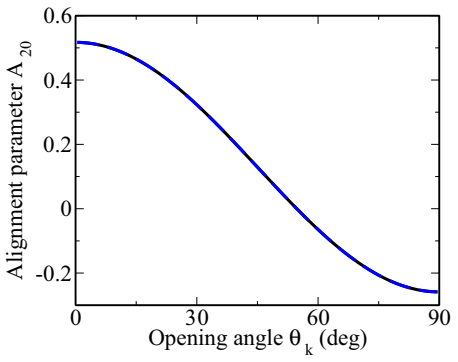

FIG. 2. (Color online) The alignment parameter $\mathcal{A}^{(1,\rm tw)}_{20}$ of the $3p\,^2P_{3/2}$ state of sodium atom following absorption of a single Bessel photon beam.

we shall focus on the parameter $\mathcal{A}^{(1,\rm tw)}_{20}(J_f = 3/2)$, which determines the angular properties of the subsequent fluorescent emission and, hence, can be observed experimentally. By making use of Eq. (26) one finds

$$\mathcal{A}^{(1,\rm tw)}_{20}(J_f = 3/2) = (1 + 3\cos 2\theta_k)\frac{a^2_{E1} + 2\sqrt{3}a_{E1}a_{M2} - a^2_{M2}}{8\left(a^2_{E1} + a^2_{M2}\right)}, \tag{27}$$

where $a_{E1} \equiv \langle 3p\,^2P_{3/2}||H_\gamma(E1)||3s\,^2S_{1/2}\rangle$ and $a_{M2} \equiv \langle 3p\,^2P_{3/2}||H_\gamma(M2)||3s\,^2S_{1/2}\rangle$ are shorthand notations for the (real) reduced matrix element of the electric dipole ($E1$) and magnetic quadrupole ($M2$) channels. To evaluate these multipole amplitudes we have applied the RATIP package [25], which helps calculate the transition probabilities and properties of many-electron atoms and ions. The alignment parameter (27) of the sodium $3p\,^2P_{3/2}$ level, excited by twisted light, is shown in Fig. 2. Result from the complete calculation, including the $M2$ amplitude, is compared with the prediction, obtained within the electric dipole approximation, when $a_{M2} = 0$. As one can expect, for a light element like sodium, both curves are virtually indistinguishable thus confirming the validity of the $E1$ approximation.

As seen from Eq. (27) and Fig. 2, the alignment of the $3p\,^2P_{3/2}$ state following absorption of the Bessel photons strongly varies with the light opening angle. For $\theta_k = 0^\circ$, for example, $\mathcal{A}^{(1,\rm tw)}_{20}(J_f = 3/2) \approx 0.5$ which coincides with the plane-wave prediction and shows the predominant population of substates with $|M_f| = 3/2$ [see Eq. (23)]. If the opening angle is enlarged, the alignment parameter decreases and even becomes negative for $\theta_k > 54^\circ$ which means that the photoabsorption mainly leads to the population of the $|M_f| = 1/2$ sublevels. Within the nonrelativistic framework a similar θ_k dependence of the magnetic sublevel population was recently found also for the $1s \rightarrow 2p$ excitation of neutral hydrogen [15].

B. Superposition of two Bessel beams

Up to now we have just discussed the magnetic sublevel population of atoms following the absorption of a single Bessel beam. As mentioned already above, experiments with a coherent superposition of *two* (or more) twisted beams with different projections of the TAM are now feasible as well. By

using Eqs. (20)–(22), we find that a simple factorization of the alignment parameters into a "plane-wave" and "twisted" part,

$$\mathcal{A}^{(2,\mathrm{tw})}_{k_f q_f}(\alpha_f J_f) = \mathcal{A}^{(\mathrm{pl})}_{k_f 0}(\alpha_f J_f) \left(\delta_{q_f,0}\, P_{k_f}(\cos\theta_k) + \sum_{n\neq n'} |c_n||c'_n|\, e^{i\,\Delta_{nn'}}\, \delta_{q_f,\, m_n - m_{n'}}\, d^{k_f}_{q_f\, 0}(\theta_k) \right), \tag{28}$$

is possible also for such superpositions of beams with $m_1 \neq m_2$. In contrast to the case (26) of a single Bessel beam, however, now also parameters $\mathcal{A}^{(2,\mathrm{tw})}_{k_f q_f}(\alpha_f J_f)$ with nonzero projection $q_f \neq 0$ may arise. Nonzero alignment parameters occur especially for $q_f = \pm\Delta m \equiv \pm|m_1 - m_2|$, i.e., if q is equal to the difference of (the projections of) two TAMs. For the given $3s$-$3p$ transition, therefore, the population of the excited $3p\,^2P_{3/2}$ state can be characterized by three alignment parameters of rank k_f, $\mathcal{A}^{(2,\mathrm{tw})}_{k_f 0}$, $\mathcal{A}^{(2,\mathrm{tw})}_{k_f q_f = m_1 - m_2}$ and $\mathcal{A}^{(2,\mathrm{tw})}_{k_f q_f = m_2 - m_1}$, if the incident light is prepared as a superposition of two Bessel beams (10) and $|m_1 - m_2| \leqslant k_f$. We later show that not all of these parameters are independent due to certain symmetry properties of the excited atom.

Let us discuss in detail the alignment parameters (28) for the $3s \to 3p$ photoexcitation of the sodium atom. In Fig. 4 we display the θ_k dependence of the second-rank tensors $\mathcal{A}^{(2,\mathrm{tw})}_{2 q_f}(\alpha_f J_f)$ as obtained for the equally weighted Bessel states, $|c_1| = |c_2| = 1/\sqrt{2}$, with phases $\alpha_1 = 0$ and $\alpha_2 = \pi/2$ [cf. Eqs. (10) and (11)]. Computations were performed, especially for a coherent superposition of two Bessel beams with the fixed value $m_1 = 1$ and with $m_2 = 2$ (upper panel), $m_2 = 3$ (middle panel), and $m_2 = 4$ (bottom panel). As one can expect from Eq. (28), the reduced tensor $\mathcal{A}^{(2,\mathrm{tw})}_{20}(J_f = 3/2)$ is independent of the projections of the TAM of twisted beams and is equivalent to the $\mathcal{A}^{(1,\mathrm{tw})}_{20}(J_f = 3/2)$ from Fig. 4 and Eq. (27). In contrast, the alignment parameters with nonzero projections, $q_f \neq 0$, are strongly affected by the variation of $\Delta m = |m_1 - m_2|$. For $\Delta m = 1$, for example, the magnetic population of the excited state $3p\,^2P_{3/2}$ level is described—apart from the alignment parameter $\mathcal{A}^{(2,\mathrm{tw})}_{20}(J_f = 3/2)$—by the two tensor components $\mathcal{A}^{(2,\mathrm{tw})}_{2,\pm 1}(J_f = 3/2)$. These purely real components become *zero* in the plane-wave limit when $\theta_k = 0$ and reach their maximum (absolute) values at $\theta_k = 45^\circ$. The nonvanishing parameters $\mathcal{A}^{(2,\mathrm{tw})}_{2,1} = -\mathcal{A}^{(2,\mathrm{tw})}_{2,-1}$ indicate that for the absorption of two Bessel beams with $\Delta m = 1$, the excited atom does not obey the axial symmetry. Such a "symmetry breaking" is caused by the transverse structure of the incident light that depends on the azimuthal angle φ_k; see Fig. 3(b).

If the difference between the projections of the TAM of two superimposed beams increases to $\Delta m = 2$, the tensors $\mathcal{A}^{(2,\mathrm{tw})}_{2,\pm 1}(J_f = 3/2)$ vanish identically but, instead, two other parameters $\mathcal{A}^{(2,\mathrm{tw})}_{2,\pm 2}(J_f = 3/2)$ become nonzero; see the middle panel of Fig. 4. As before, these purely imaginary parameters are zero for $\theta_k = 0^\circ$ and are related to each other as $\mathcal{A}^{(2,\mathrm{tw})}_{2,2}(J_f = 3/2) = -\mathcal{A}^{(2,\mathrm{tw})}_{2,-2}(J_f = 3/2)$. If Δm is further enlarged, $\Delta m > 2$, only a single alignment parameter

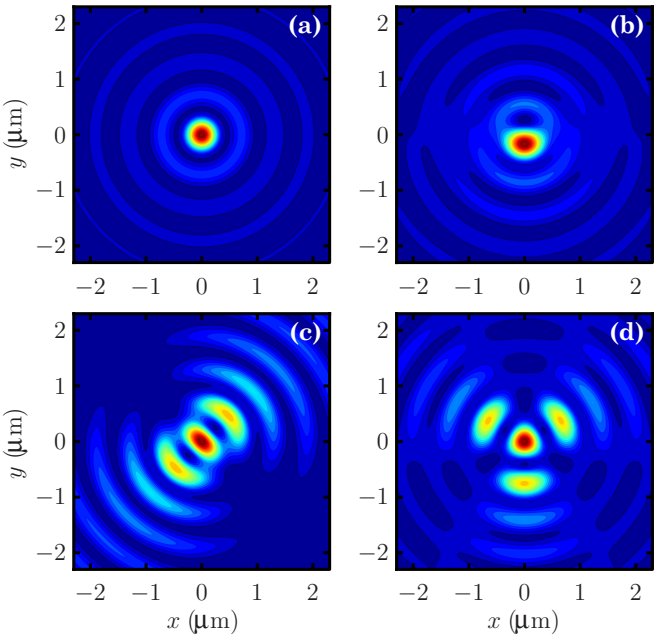

FIG. 3. (Color online) Transverse energy density profile $\rho(x,y)$ of various Bessel beams and with different projections m of the TAM. (a) Single beam with $m_1 = 1$; (b) coherent superposition of two equally weighted beams with $m_1 = 1$ and $m_2 = 2$; (c) the same as (b) but for $m_1 = 1$ and $m_2 = 3$; (d) the same as (b) but for $m_1 = 1$ and $m_2 = 4$. Results are presented in arbitrary units, and for the opening angle $\theta_k = 45^\circ$, photon energy $\hbar\omega = 2.104$ eV and phases $\alpha_1 = 0, \alpha_2 = \pi/2$.

$\mathcal{A}^{(2,\mathrm{tw})}_{20}(J_f = 3/2) = \mathcal{A}^{(1,\mathrm{tw})}_{20}(J_f = 3/2)$ is *nonzero*. For such superposition of beams, the axial symmetry of the residual atom is "restored" as for the case of a single Bessel beam. This symmetry is observed despite the fact that the transverse structure of the incident light is strongly φ_k–dependent [see Fig. 3(d)]. The parameters $\mathcal{A}^{(2,\mathrm{tw})}_{2 q_f}(J_f = 3/2)$ with $q_f \neq 0$ vanish because of the selection rules $q_f = \pm|m_1 - m_2|, q_f = -k_f, \ldots k_f$ in Eq. (28). In order to "see" the TAM's difference of $\Delta m > 2$ one would need to consider the reduced statistical tensors $\mathcal{A}^{(2,\mathrm{tw})}_{k_f q_f}$ of some higher rank, $k_f > 2$. Such tensors arise if atomic levels with $J_f > 3/2$ are excited. Analysis of the transitions to such higher-lying levels is out of the scope of the present paper and will be presented elsewhere.

The variation of the alignment parameters $\mathcal{A}^{(2,\mathrm{tw})}_{2 q_f}(J_f = 3/2)$ with the opening angle θ_k and the difference Δm of the projections of the TAM can be reflected in the angular distribution (24) of the subsequent fluorescent photons. For the $3p\,^2P_{3/2} \to 3s\,^2S_{1/2}$ fluorescence line of sodium atom following the photoabsorption, this angular distribution is given by

$$W_{\mathrm{dec}}(\theta) = \frac{1}{4\pi}\Big[1 + \frac{1}{32}\,\mathcal{A}^{\mathrm{pl}}_{20}(J_f = 3/2) \times \big((1 + 3\cos 2\theta_k)(1 + 3\cos 2\theta) + \delta_{\Delta m,1}\,|c_1||c_2|\,12\sin 2\theta_k \sin 2\theta \sin(\alpha_1 - \alpha_2) - \delta_{\Delta m,2}\,|c_1||c_2|\,12\sin^2\theta_k \sin^2\theta \cos(\alpha_1 - \alpha_2)\big)\Big], \tag{29}$$

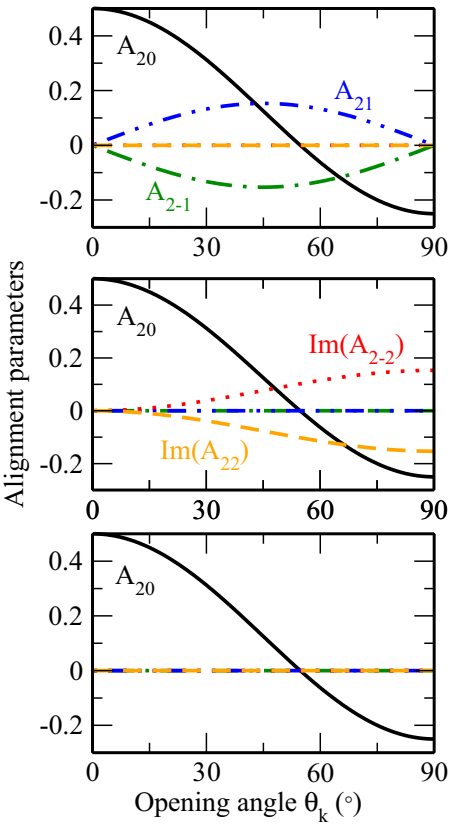

FIG. 4. (Color online) The alignment parameters $\mathcal{A}^{(2,\mathrm{tw})}_{2q_f}$ of the $3p\,^2P_{3/2}$ state of sodium atom following the absorption of a twisted light. Calculations were performed for a coherent superposition of two equally weighted beams with fixed value $m_1 = 1$ for the first beam and the different values of the TAM projection of the second beam: $m_2 = 2$ (upper panel), $m_2 = 3$ (middle panel) and $m_2 = 4$ (bottom panel).

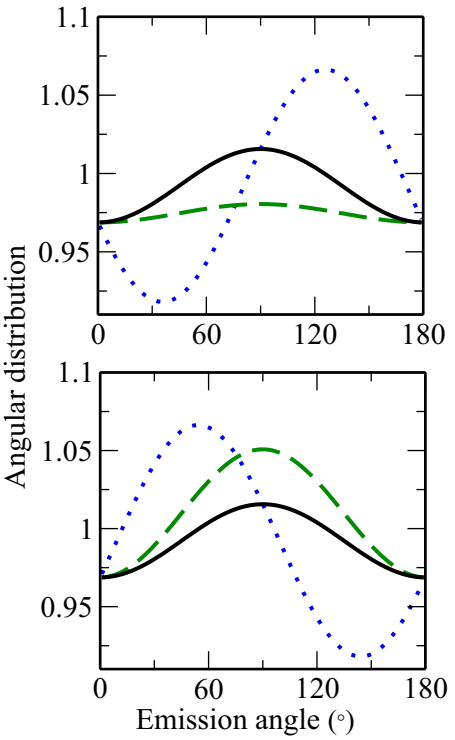

FIG. 5. (Color online) The angular distribution of the $3p\,^2P_{3/2} \rightarrow 3s\,^2S_{1/2}$ fluorescence light following the photoexcitation of sodium atoms by a coherent superposition (10) of two Bessel beams. The beams are prepared in the state with the opening angle $\theta_k = 60^\circ$, the phases $\alpha_1 = 0$ and $\alpha_2 = \pi/3$ (upper panel), as well as $\alpha_1 = 0$ and $\alpha_2 = 4\pi/3$ (bottom panel), and with the projections of the total angular momentum $m_1 = 1$ and $m_2 = 2$ (dotted line), $m_2 = 3$ (dashed line), and $m_2 = 4$ (solid line).

where we made use of Eq. (28) and where we have restricted ourselves to the electric-dipole approximation for the structure function (25). In Fig. 5, we display the angular distribution $W_{\mathrm{dec}}(\theta)$ for the opening angle $\theta_k = 60^\circ$ of the incident twisted light, and for $\Delta m = 1$ (dotted line), $\Delta m = 2$ (dashed line), and $\Delta m = 3$ (solid line). Moreover, we have assumed two equally weighted Bessel beams with phase factors $\alpha_1 = 0$ and $\alpha_2 = \pi/3$ (upper panel), as well as $\alpha_1 = 0$ and $\alpha_2 = 4\pi/3$ (bottom panel). As seen from the figure, the angular distribution (29) of the fluorescent radiation, measured within the reaction plane, appears to be very sensitive to (the difference of) both the TAM projections, Δm, and the phases, $\Delta\alpha = \alpha_1 - \alpha_2$, of two Bessel states. In particular, for $\Delta m = 1$ the $W_{\mathrm{dec}}(\theta)$ is strongly anisotropic and peaks at $\theta = 125.8^\circ$ and $\theta = 61.1^\circ$ for $\Delta\alpha = -\pi/3$ and $\Delta\alpha = -4\pi/3$ respectively. If the difference between the projections of the TAM of two Bessel beams changes to $\Delta m = 2$, the decay photons are emitted predominantly perpendicular to the quantization axis, and the effect becomes most pronounced for $\alpha_2 = 4\pi/3$. A symmetric—with respect to the polar angle $\theta = 90^\circ$—angular distribution can be observed also for the $\Delta m = 3$. In this case, however, the $W_{\mathrm{dec}}(\theta)$ just reproduces the emission pattern of the fluorescent light following absorption of a *single* Bessel beam and is independent of the phase and TAM differences. The same pattern, which is influenced only by the opening angle θ_k, will be also observed for any larger difference $\Delta m > 3$.

The Δm dependence of the $W_{\mathrm{dec}}(\theta)$ can be used, for example, to determine the TAM projection of an unknown Bessel beam if it is coherently mixed with a "reference" beam whose m is well known. Similar information can be obtained also from the measurement of the linear polarization of the fluorescence light. For the sake of brevity we shall not discuss here such a polarization and just mention that it is uniquely defined by the set of alignment parameters $\mathcal{A}^{(2,\mathrm{tw})}_{2q_f}$ and, hence, by the difference in the TAM projections of the two beam components.

IV. SUMMARY AND OUTLOOK

The density-matrix theory has been applied to investigate the excitation of atoms (or ions) by twisted light. Special emphasis was placed on the magnetic sublevel population of the excited atomic states, that is usually described in terms of the alignment parameters $\mathcal{A}_{k_f q_f}$. In particular, we have derived a general expression for the $\mathcal{A}_{k_f q_f}$ if we had assumed that the incident photon beam is prepared as a coherent superposition of *two* Bessel beams and that it collides with a *macroscopic* target. This expression depends neither on the number of

electrons nor on particular shell structure of target atoms and fully accounts for the higher-order multipoles of the radiation field. From the analysis of the alignment parameters we found that the population of photoexcited atomic states can be very sensitive not only with regard to the kinematic parameters of the Bessel beams, such as the ratio of transverse $\varkappa$ to longitudinal k_z momenta, but also to their relative phase and the difference of the projections of the total angular momenta. It was shown, moreover, how the parameters of the (incident) twisted radiation affects also the angular distribution of the subsequent decay photons.

While the formalism developed here can be employed to study the photoexcitation of *any* atom, detailed calculations have been performed for the $3s\,^2S_{1/2}(J_i = 1/2) + \gamma \to 3p\,^2P_{3/2}(J_f = 3/2)$ transition in neutral sodium. For this transition, we paid particular attention to the second-rank alignment parameters $\mathcal{A}_{2q_f}(J_f = 3/2)$ which uniquely define the emission pattern of the fluorescence radiation. We have shown that the parameter $\mathcal{A}_{20}(J_f = 3/2)$ with *zero* projection q_f depends only on the opening angle $\theta_k = \arctan(\varkappa/k_z)$ of the incident beams but is otherwise insensitive to their TAM projections m_1 and m_2. In contrast, the reduced tensors $\mathcal{A}_{2q_f}(J_f = 3/2)$ with $q_f \neq 0$ can be strongly affected by the difference $\Delta m = \pm|m_1 - m_2|$ of the total angular momenta as well as by the relative phase of the Bessel states. This dependence on the "twistedness" of incoming radiation can be extracted from the angular distribution of the subsequent $3p\,^2P_{3/2} \to 3s\,^2S_{1/2}$ decay. Experimental observations of the $3p$-$3s$ fluorescence photons are well established today and can provide, therefore, valuable information about the interaction of twisted light with atomic ensembles.

In the present study we have evaluated the alignment of the (photo)excited atomic states for the case where the size of the target is much *larger* compared to the cross section of the incident photon beam. Owing to the recent advances in trapping and optical lattice technologies, however, experiments with *microscopic* atomic (or ionic) targets may become feasible in the near future. If the transverse extension of such targets will be comparable to the characteristic scale of the Bessel beams, one then expects a rather complicated dependence of the magnetic sublevel population of excited atoms on the parameters of twisted light. A more detailed analysis of this dependence is currently underway and will be presented elsewhere.

ACKNOWLEDGMENTS

The work was supported by the ExtreMe Matter Institute (EMMI). V.G.S. acknowledges support from RFBR (via Grant No. 13–02–00695), NSh–3802.2012.2, and MES (Russia).

[1] G. Molina-Terriza, J. P. Torres, and L. Torner, Nat. Phys. **3**, 305 (2007).
[2] A. M. Yao and M. J. Padgett, Adv. Opt. Photon. **3**, 161 (2011).
[3] J. P. Torres and L. Torner, *Twisted Photons: Applications of Light with Orbital Angular Momentum* (Wiley-VCH, Weinheim, 2011).
[4] H. He, M. E. J. Friese, N. R. Heckenberg, and H. Rubinsztein-Dunlop, Phys. Rev. Lett. **75**, 826 (1995).
[5] G. F. Quinteiro and P. I. Tamborenea, Europhys. Lett. **85**, 47001 (2009).
[6] J. F. S. Brachmann, W. S. Bakr, J. Gillen, A. Peng, and M. Greiner, Opt. Express **19**, 12984 (2011).
[7] A. Picòn, A. Benseny, J. Mompart, J. R. Vózquez de Aldana, L. Plaja, G. F. Calvo, and L. Roso, New J. Phys. **12**, 083053 (2010).
[8] O. Matula, A. G. Hayrapetyan, V. G. Serbo, A. Surzhykov, and S. Fritzsche, J. Phys. B **46**, 205002 (2013).
[9] B. S. Davis, L. Kaplan, and J. H. McGuire, J. Opt. **15**, 035403 (2013).
[10] P. Guthrey, L. Kaplan, and J. H. McGuire, Phys. Rev. A **89**, 043826 (2014).
[11] U. D. Jentschura and V. G. Serbo, Phys. Rev. Lett. **106**, 013001 (2011).
[12] A. Afanasev, C. E. Carlson, and A. Mukherjee, Int. J. Mod. Phys.: Conf. Ser. **25**, 1460048 (2014).
[13] A. Afanasev, C. E. Carlson, and A. Mukherjee, Phys. Rev. A **88**, 033841 (2013).
[14] A. Afanasev, C. E. Carlson, and A. Mukherjee, J. Opt. Soc. Am. B **31**, 2721 (2014).
[15] H. M. Scholz-Marggraf, S. Fritzsche, V. G. Serbo, A. Afanasev, and A. Surzhykov, Phys. Rev. A **90**, 013425 (2014).
[16] K. Blum, *Density Matrix Theory and Applications* (Plenum, New York, 1996).
[17] V. V. Balashov, A. N. Grum-Grzhimailo, and N. M. Kabachnik, *Polarization and Correlation Phenomena in Atomic Collisions* (Kluwer Academic/Plenum Publishers, New York, 2000).
[18] A. I. Akhiezer and V. B. Berestetskii, *Quantum Electrodynamics* (Interscience, New York, 1965).
[19] I. P. Grant, J. Phys. B **7**, 1458 (1974).
[20] M. E. Rose, *Elementary Theory of Angular Momentum* (John Wiley & Sons, New York, 1957).
[21] A. Surzhykov, S. Fritzsche, and Th. Stöhlker, J. Phys. B **35**, 3713 (2002).
[22] S. Fritzsche, A. Surzhykov, and Th. Stöhlker, Phys. Rev. A **72**, 012704 (2005).
[23] A. Surzhykov, U. D. Jentschura, Th. Stöhlker, and S. Fritzsche, Phys. Rev. A **73**, 032716 (2006).
[24] O. Matula, S. Fritzsche, and A. Surzhykov, J. Phys. B **45**, 215004 (2012).
[25] S. Fritzsche, Comput. Phys. Commun. **183**, 1525 (2012).